

## Fabrication Technology of the Focusing Grating Coupler using Single-step Electron Beam Lithography

Tae-Youb Kim\*, Yark-Yeon Kim, Gee-Pyeong Han, and Mun-Cheol Paek  
*Data Storage Device Team, Advanced Micro-Electronics Research Laboratory Electronics and  
Telecommunications Research Institute, 161 Gajeong-Dong, Yusong-Gu, Taejon 305-350, Korea.*

Hae-Sung Kim, Byeong-Ok Lim, Sung-Chan Kim, Dong-Hoon Shin, and Jin-Koo Rhee  
*Millimeter-wave Innovation Technology Research Center, Dongguk University,  
Seoul 100-715, Korea.*

E-mail : youby@etri.re.kr

(Received 4 December 2001, Accepted 6 February 2002)

A focusing grating coupler (FGC) was not fabricated by the 'Continuous Path Control' writing strategy but by an electron-beam lithography system of more general exposure mode, which matches not only the address grid with the grating period but also an integer multiple of the address grid resolution (5 nm). To more simplify the fabrication, we are able to reduce a process step without large decrease of pattern quality by excluding a conducting material or layer such as metal (Al, Cr, Au), which are deposited on top or bottom of an e-beam resist to prevent charge build-up during e-beam exposure. A grating pitch period and an aperture feature size of the FGC designed and fabricated by e-beam lithography and reactive ion etching were ranged over 384.3 nm to 448.2 nm, and  $0.5 \times 0.5 \text{ mm}^2$  area, respectively. This fabrication method presented will reduce processing time and improve the grating quality by means of a consideration of the address grid resolution, grating direction, pitch size and shapes when exposing. Here our investigations concentrate on the design and efficient fabrication results of the FGC for coupling from slab waveguide to a spot in free space.

*Keywords* : Focusing grating coupler, Electron-beam lithography,  $\text{Si}_3\text{N}_4$ , Dry etching

### 1. INTRODUCTION

A focusing grating coupler (FGC) has been developed for application to optical data storage and also has the potential to play an important role in a variety of integrated optics applications[1-5] such as guiding to LD or fiber couplers and integrated optic disk pickup devices because of its ability to couple light into and out of a waveguide. As a rule, the FGC's structure can be described by the change in the (relative) dielectric permittivity  $\Delta\epsilon$  caused by the grating in the fundamental waveguide structure. The matter of controlling very small grating linewidth and achieving an extremely high quality in the desirable ratio of line and space as well as a high degree of quality for line edges is arguably the single most important lithographic technology in manufacturing the micro-optical elements with the properties of beam steering, coupling, multi-division and optic disk data pickup applications[6-9]. The first effort of adding a complex wavefront conversion to a grating

coupler was in waveguide holograms, which aimed at an approach to hologram integration[7,10,11]. A pictorial

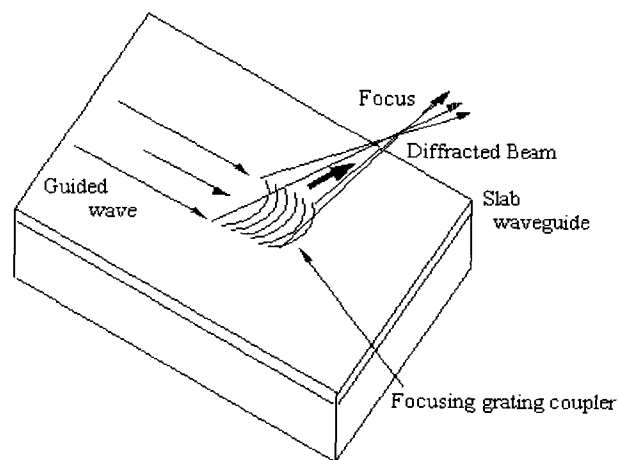


Fig. 1. A focusing grating coupler configuration.

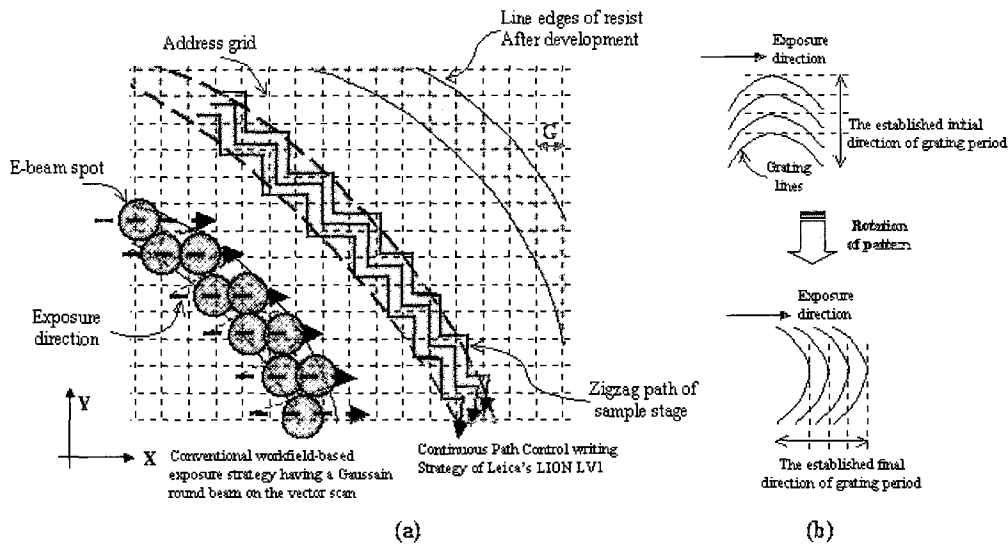


Fig. 2. Basic scheme of (a) the CPC and the conventional workfield-based exposure strategy on the vector scan and (b) the transformation strategy on the design and fabrication of the grating pattern.

image was recorded by interference and re-constructed by a guided wave. A special example of waveguide holograms is a focusing grating coupler[12], as shown in Fig. 1, where the object is a point image.

The FGC's were fabricated by the holographic technique. However, they exhibited large aberrations, except for ones with a small aperture, due to the difference in wavelength between the fabrication and coupling lights[13]. It has been possible that the e-beam writing makes an aberration-free FGC's, and gives an extremely high quality in the desirable ratio of line and space[14,15].

The accuracy of the grating coupler fabricated is strongly related to the properties of electron beam lithography tools used when exposing[16,17]. As a rule, to fabricate a curved and chirped grating such as a polygonal or spiral pattern varying pitch and curvature (e.g. arcs, circles), Leica's LION LV1 for the 'Continuous Path Control' (CPC) writing strategy type [17,18] has remained a strong candidate of embossing techniques suitable for fabricating grating elements. The sample stage of this tool especially moves continuously along a given path while the e-beam maintains undeflected. Thus the stage movement is controlled by using some spline (Bézier spline)[17] enabling the exposure of straight or arbitrarily curved lines, as shown in Fig. 2, where the example shows the curved exposing line (for clarity purposes, the scale in Fig. 2 is supposed, and address grid size  $G$  is actually much smaller than linewidth and grating period.). However, during the e-beam exposure this tool (Leica's LION LV1) also has a well-known error (stitching errors and butting errors) such as grating ghosts formed due to the influence of the

address grid (for the e-beam writer, the address grid is the main property influencing the grating quality), according to large-area gratings or bad layout grating pattern. In analyzing and evaluating the relation between fabrication and optical grating quality, some important things are the performance, types and kinds of the e-beam writer, but more important things are an arbitrary type and direction of pattern laid out and designed as follows; to suppress grating ghosts and decrease fabrication errors, the grating period has to be an integer multiple of the address grid size  $G$  matching the one with the address grid. Therefore in common workfield-based exposure systems taking into account the above things, we report that the gratings quality can be sufficiently improved in experiment. Here, the e-beam lithography system used is a Leica Microsystems Lithography Ltd Electron beam Pattern Generator (EBPG-4HR) with most conventional workfield-based exposure strategies having a Gaussian round beam on the vector scan. Meanwhile, our system includes both positioning things: positioning the beam within a limited area (workfield) by means of the electromagnetic beam deflection inside the e-beam column, and the positioning of the several workfields on the sample by means of moving the sample stage[19,20]. For more accurate fabrication of such optical grating and pattern with arbitrary periods, a research for reducing the address grid to the sub-Angström region and developing the more safe system is necessary preferentially.

The aim of this article is to present the fabrication technologies and each of process steps in experiment for the focusing grating coupler, which is one of versatile passive components for integrated optics, and reports

further results on electron-beam exposure mode or strategy to most effectively fabricate the FGC using single-step electron beam lithography.

## 2. FABRICATION TECHNOLOGY

The key to realize successful FGC's performance lies in the uniformity and reproducibility of the grating formation process and fabrication, coupled intimately with the materials properties (each of layer thickness, refractive index, the relative dielectric permittivity, doping, charge density, etc.). Our group has described fabrication sequence of the grating earlier, but this tends to be quite generic in principle. Here we discuss steps of the grating formation process that are relevant to the topic at hand.

### 2.1 Materials properties and grating patterning

The specification of FGC's are summarized in Table 1. The FGC was fabricated in the following manner. On a 10.16-cm (4-in.) silicon (100) substrate four layers were deposited: a buffer layer (SiO<sub>2</sub>, thickness = 1 μm, refractive index = 1.459) by thermal oxidation in furnace, a cladding layer (Cladding #7740 glass, 2.5 μm, 1.473) by RF sputtering (plate temperature = 573 K, RF-power = 210 W), a waveguide (core) layer (BK7 & BAK4 glass, 1 μm, refractive index = 1.515, 1.5667, respectively) by RF sputtering (plate temperature = 573 K, RF-power = 210 W), a grating layer (Si<sub>3</sub>N<sub>4</sub>, 0.15 μm, 1.78) by plasma-enhanced CVD (PECVD) techniques (such

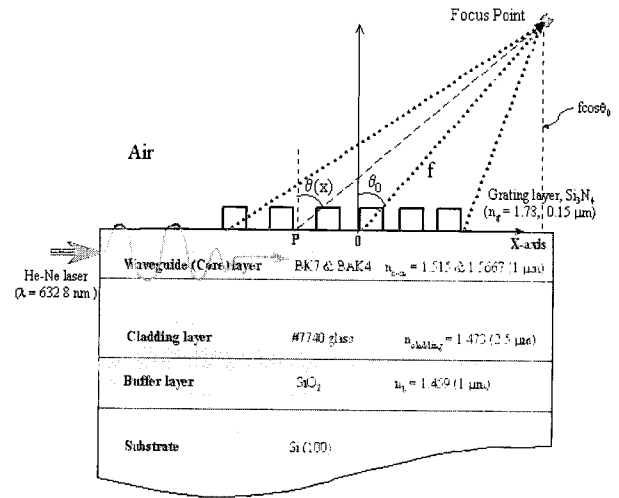


Fig. 3. Schematic illustration of the proposed FGC' s structure.

plasma deposited nitrides are really polymer-like Si-N-H materials). A schematic cross-section view of the FGC' s structure is given in Fig. 3. The total working specimen area was 25 × 25 mm<sup>2</sup>.

We sequentially report optimum fabrication conditions that a high-periodicity FGC with the focusing beam in air as shown in Fig. 3 were investigated and fabricated by e-beam lithography in Si<sub>3</sub>N<sub>4</sub> (0.15 μm)/glass (3.5 μm)/SiO<sub>2</sub> (1 μm)/Si (100) waveguide. A 2.0 μm line and

Table 1. Specification of the fabricated FGC.

	Parameter	Measurement
Light Source	HeNe laser (wavelength)	$\lambda = 632.8 \text{ nm}$
Waveguide		
Grating layer	Si <sub>3</sub> N <sub>4</sub>	$n_g = 1.78 (0.15 \text{ } \mu\text{m})$
Core layer	BK7 & BAK4	$n_{\text{core}} = 1.515 \text{ \& } 1.5667 (1 \text{ } \mu\text{m})$
Cladding layer	#7740 glass	$n_{\text{cladding}} = 1.473 (2.5 \text{ } \mu\text{m})$
Buffer layer	SiO <sub>2</sub>	$n_b = 1.459 (1 \text{ } \mu\text{m})$
Substrate	Si (100)	
FGC's		
Aperture		$0.5 \times 0.5 \text{ mm}^2$
Output angle		$\theta_0 = 15^\circ$
Grating pitch	period	$\Lambda = 384.3 \sim 448.2 \text{ nm}$

space grating coupler patterned on a specimen of Si<sub>3</sub>N<sub>4</sub> (0.15 μm)/ Si (substrate) was done by electron beam lithography using a Leica Microsystems Lithography Ltd Electron beam Pattern Generator (EBPG-4HR system) operating at an acceleration voltage of 50 kV, a beam spot size of 50 nm and a probe current (beam current) of 800 pA for a thermionic LaB<sub>6</sub> filament emitter. We have just used two layers of Si<sub>3</sub>N<sub>4</sub> (0.15 μm)/Si (substrate) to test the grating pattern on a silicon nitride layer. The specifications applied on the EBPG-4HR system used in experiment are given in Table 2.

Table 2. Specification of EBPG-4HR which was used with experiment in electron beam lithography.

Specification conditions of EBPG-4HR	
Accelerating voltage of electron beam (EHT)	50 [kV]
Probed beam current	800 [pA]
Beam step size/Resolution	50/50 [nm]
Beam spot size	50 [nm]
Field size	800 × 800 [μm <sup>2</sup> ]
Beam shape	Gaussian beam shape
Exposure scan method	Vector scan
Overlay accuracy	Less than 80 nm

Before achieving suitable resist profiles of the gratings with an overhang or vertical structure for a fine RIE process, a few dose tests and optimum resist thickness are necessary. In the e-beam writing, there are some effects such as charging effect resulting in pattern distortion and alignment errors, and proximity effect as a result of producing a backward and forward electron scattering[21,22] and secondary electrons, according as the resist thickness and the dose are increased[23-25]. As a result, the gratings patterned have an over-exposed phenomenon. Another problems on the fabrication related to pattern qualities are well-known errors (overlay or stitching and butting errors) such as grating ghosts formed due to the influence of the address grid (for the e-beam writer, the address grid is the main property influencing the grating quality)[17], according to large-area gratings or bad layout grating pattern. To resolve these problems, firstly, the resist thickness needs to be reduced as thin as possible. Therefore we produced a small resist thickness of 2000 Å to define a grating layer by using an e-beam resist of polymethylmethacrylate (PMMA 950 K 4% resist, refractive index =

1.49) and a compatible coating speed of 7000 rpm, and also found an appropriate dose of 350 μC/cm<sup>2</sup> as a result of conducting the exposure dose test, ranging from 200 to 700 μC/cm<sup>2</sup> in 50 μC/cm<sup>2</sup> increments. A MIBK : IPA solution of (1:3) was used to develop the patterned resist using both spray and immersion. Development times ranged from 60 to 660 seconds in 20-second increments. A variation of PMMA thickness after coating according to the spin speed is given in Fig. 4.

The fabrication process of grating pattern is depicted in Fig. 5. To more simplify the fabrication and improve the grating quality, secondly, we have applied the same exposure strategies that the grating period has to be an integer multiple of the address grid size, and that match the one with the address grid by rotating the total grating pattern to 90 degrees.

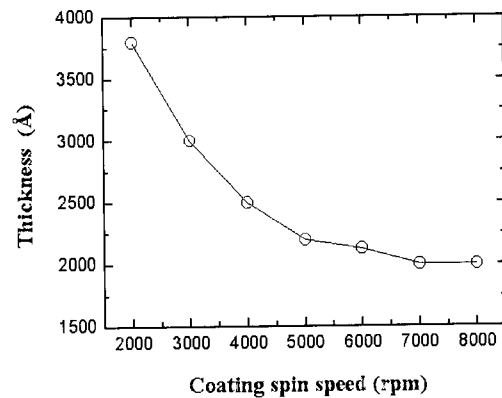


Fig. 4. Resist (PMMA 950 K, 4 %) thickness as a function of the coating spin-speed.

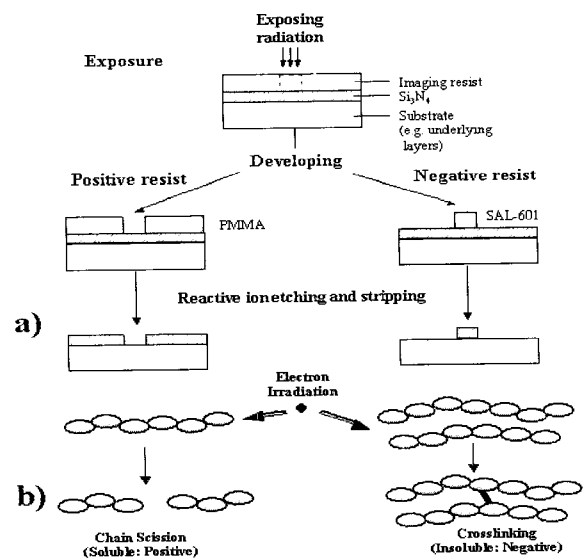


Fig. 5. Schematic illustration of the FGC process (a) e-beam patterning, etching and (b) chain scission and crosslinking mechanism.

Therefore each of the curved gratings lies on the perpendicular to the x-axis when taking account of a two-dimensional plane. This x-axis is an e-beam exposure direction and the address grid axis simultaneously. The SEM micrograph of line profiles of PMMA with a half grating pitch width of  $0.2\ \mu\text{m}$  between line and space at a constant development time of 120 s, after

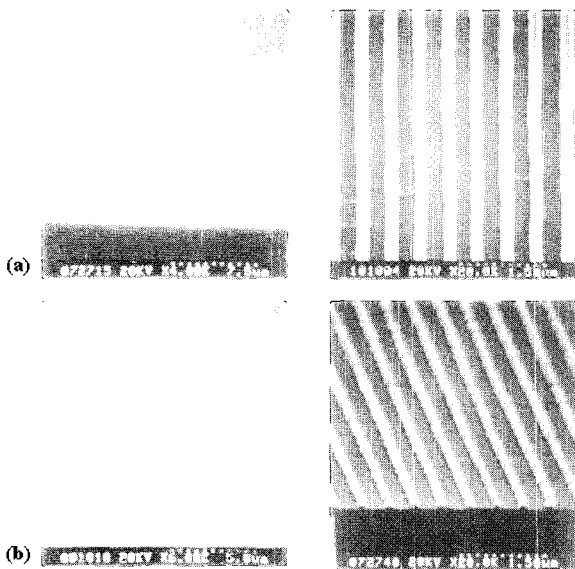


Fig. 6. SEM micrograph of the gratings fabricated with (a) rotating the pattern to 90 degrees (b) without rotating.

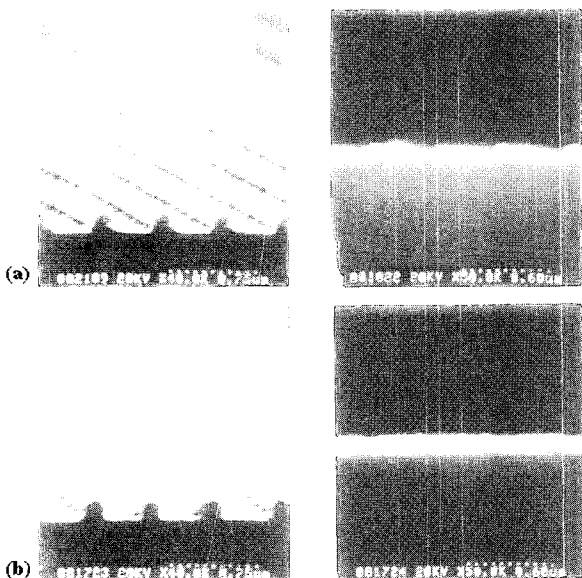


Fig. 7. SEM micrograph showing a cross-sectional view of the grating lines fabricated with (a) rotating the pattern to 90 degrees (b) without rotating.

Patterning in a normal state without a rotation and in a rotation state of 90 degrees, is given in Fig. 6 and 7, respectively.

Here, we achieved the improved grating quality on optimum fabrication and design conditions through these experiments.

## 2.2 Dry etching

Due to its anisotropic etching characteristics, reactive ion etching (RIE) is the most frequently used dry etching technique in the microfabrication of semiconductor devices[26]. As a rule, it is essential for this technique that the wafers are electrically contacted with one of the internal electrodes, and the inner pressure of the chamber is low (below 10 Pa). As the wafers are contacted with one of the electrodes, the ambient condition on the surface of the wafer is the same as that of the electrode. Because of a large difference in mobility between electrons and ions, an ion-rich layer called an ion sheath is formed on both of the surfaces. At the time when the surfaces of wafer and electrode are negatively charged, a large difference in electric potential arises across the ion sheath. By the gradient of potential, ions in the ion sheath are accelerated perpendicularly to the surface of the wafer. In the case of the relatively low working pressure, as the etching reaction is significantly accelerated by the impact of incident ions, the etching proceeds anisotropically[27].

To achieve more agreeable grating profiles and qualities using these anisotropic etching characteristics, we previously examined the practical etching conditions of finding an appropriate etching time, etching rate and the etching status according to RF power, working pressure and gas flow rate used in RIE. Here, the gas used to define a  $\text{Si}_3\text{N}_4$  layer was a fluorine-containing gaseous compound such as carbon tetrafluoride ( $\text{CF}_4$ ) [20,27]. Therefore we achieved the optimum-etching conditions as follows: a defined layer ( $\text{Si}_3\text{N}_4$ ), gas composition (100 %  $\text{CF}_4$ ), gas flow rate (50 sccm), RF power (100 W), DC power voltage (-394 V), working pressure (50 mTorr), etching time (4 min), etching rate ( $395\ \text{\AA}/\text{min}$ ). Fig. 8 shows the SEM micrograph of grating profiles and a cross-section view of lines with a half grating pitch width of  $0.2\ \mu\text{m}$  between line and space, after etching [31-33].

## 3. RESULTS AND DISCUSSION

To minimize the errors on the FGC fabrication (a grating formation part) that may affect all of the optical characteristics such as a coupling efficiency, radiation directionality and focusing performance, we examined the influence of occurring the grating pattern quality by means of exposure modes, strategies and orientation

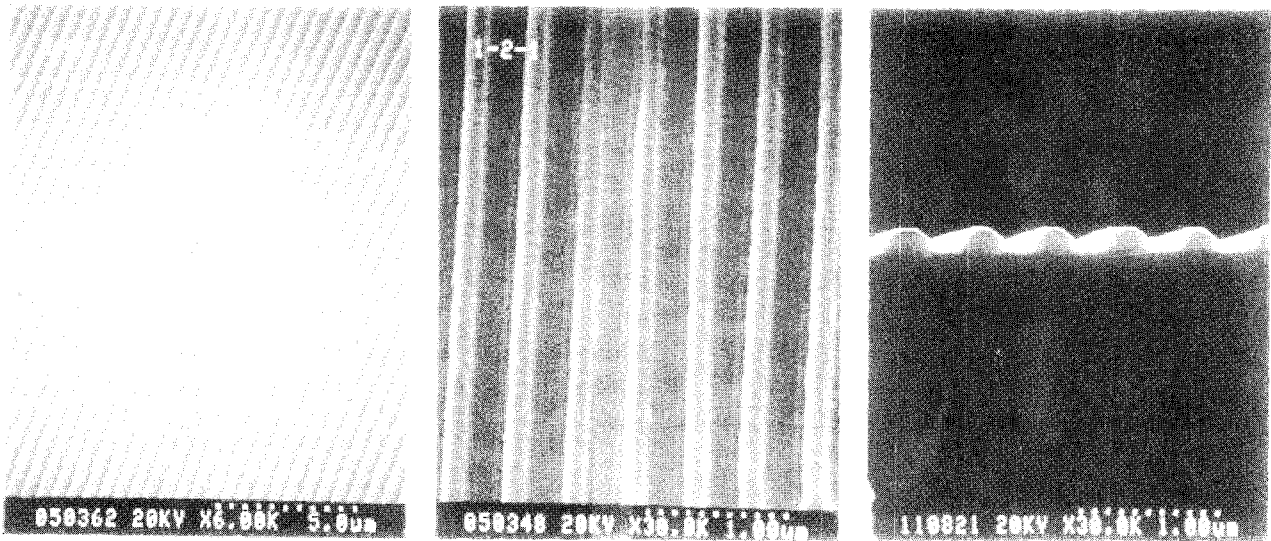


Fig. 8. SEM micrograph of grating profiles and a cross-section view of lines with a half grating pitch width of 0.2  $\mu\text{m}$  between line and space, after etching.

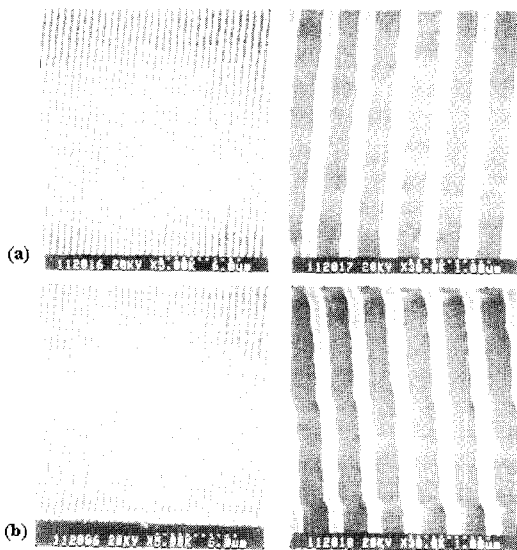


Fig. 9. Micrographs of a non-distorted (a) and a distorted (b) grating pattern.

directions on the pattern through the conventional e-beam lithography machine (EBPG-4HR: with a Gaussian round beam of the vector scan type) without using the LION LV1 e-beam writer of the Continuous Path Control (CPC) exposure mode. As a result, we obtained the information that a constant or varying period of grating and dot pattern quality could sufficiently be improved with setting an appropriate exposure strategy and pattern design through these experiments, which are able to apply not only the LION LV1 e-beam writer of the CPC exposure mode but also most of the conventional e-beam



Fig. 10. SEM photograph showing a difference in the pattern quality, which was generated on a SAL-601 resist defined with (a) rotating the grating pattern to 90 degrees (b) without rotating.

lithography machines [17,28-30].

Two things were applied as follows: designed to be an integer multiple of the address grid size  $G$  and matched the address grid with the grating period by rotating the total grating pattern to 90 degrees. Experiment results taking into account the above things or not were different significantly, as shown in Fig. 6, 7, and 9. Figure 10 also the SEM micrograph of line profiles for an e-beam negative resist of SAL-601 after patterning, which include a 90-degree rotation or not. We think that resist types, resist properties and fabrication condition (dose, bake, development, temperature, humidity etc.) actually

affect the pattern qualities during the e-beam patterning, but indeed, it is further important to consider pattern design and exposure strategy such as pattern shapes, their orientation direction, resolution, address grid size, etc., which are related to the e-beam tool's performance.

#### 4. CONCLUSION

A curved grating pattern with a half grating pitch width of 0.2  $\mu\text{m}$  between line and space has been successfully fabricated by single-step electron beam lithography and reactive ion etching. We were able to understand the influence according to the transformation on the design and fabrication of the grating pattern, and also obtain optimum fabrication condition of the gratings. We think that the previously described approach which combined the advantages of reducing the patterning errors and the improvement of the pattern quality by adapting the grating period to the address grid resolution will lead to possible other integrated optic-device fabrications and applications.

#### ACKNOWLEDGEMENT

This work was supported by Electronics and Telecommunications Research Institute (ETRI) and KOSEF under the ERC program through the Millimeter-wave INnovation Technology (MINT) research center at Dongguk University in Seoul, Korea.

#### REFERENCES

- [1] Y. Ito, A. L. Bleloch, and L. M. Brown, "Nanofabrication of solid-state Fresnel lenses for electron optics", *Nature*, Vol. 394, p. 49, 1998.
- [2] P. Yang, G. Wirthsberger, H. C. Huang, S. R. Cordero, M. D. McGehee, B. Scott, and T. Deng, "Mirrorless lasing from mesostructured waveguides patterned by soft lithography", *Science*, Vol. 287, p. 465, 2000.
- [3] M. Li, J. C. H. Lin, M. J. Cherrill, and S. J. Sheard, "Fabrication of submicrometre parallelogram-shaped grating in  $\text{SiO}_2$ ", *Electron. Lett.*, Vol. 30, p. 2126, 1994.
- [4] R. Waldhäusl, B. Schnabel, E.-B. Kley, and A. Brauer, "Efficient focusing polymer waveguide grating couplers", *Electron. Lett.*, Vol. 33, p. 623, 1997.
- [5] S. M. Schultz, E. N. Glytsis, and T. K. Gaylord, "Volume grating preferential-order focusing waveguide coupler", *Opt. Lett.*, Vol. 15, p. 1708, 1999.
- [6] S. Ura, T. Suhara, and H. Nishihara, "Aberration characterizations of a focusing grating coupler in an integrated-optic disk pickup device", *Appl. Opt.*, Vol. 26, p. 4777, 1987.
- [7] T. Suhara and H. Nishihara, "Integrated optics components and devices using periodic structures", *IEEE J. Quantum Electron.*, Vol. QE-22, p. 845, 1986.
- [8] S. Sheard and T. Suhara, "Integrated-optic implementation of a confocal scanning optical microscope", *IEEE J. Lightwave Technol.*, Vol. 11, No. 8, p. 1400, 1993.
- [9] I. Kawakubo, J. Funazaki, K. Shirane, and A. Yoshizawa, "Integrated optical-disk pickup that uses a focusing grating coupler with a high numerical aperture", *Appl. Opt.* Vol. 33, p. 6855, 1994.
- [10] T. Suhara, H. Nishihara, and J. Koyam, "Waveguide holograms: A new approach to hologram integration", *Opt. Commun.*, Vol. 19, p. 353, 1976.
- [11] G. Hatakoshi, H. Fujima, and K. Goto, "Waveguide grating lenses for optical couplers", *Appl. Opt.*, Vol. 23, p. 1749, 1984.
- [12] P. J. Cronkite and G. N. Lawrence, "Focusing grating coupler design method using holographic optical elements", *Appl. Opt.*, Vol. 27, p. 679, 1988.
- [13] R. Waldhäusl, B. Schnabel, and P. Dannberg, "Efficient coupling into polymer waveguides by gratings", *Appl. Opt.*, Vol. 36, p. 9383, 1997.
- [14] G. N. Lawrence and P. J. Cronkite, "Physical optics analysis of the focusing gratings coupler", *Appl. Opt.*, Vol. 27, p. 672, 1988.
- [15] J. Seligson, "Modeling of a focusing grating coupler using vector scattering theory", *Appl. Opt.*, Vol. 27, p. 684, 1988.
- [16] T. Ito and S. Okazaki, "Pushing the limits of lithography", *Nature*, Vol. 406, p. 31, 2000.
- [17] B. Schnabel and E.-B. Kley, "On the influence of the e-beam writer address grid on the optical quality of high-frequency gratings", *Microelectron. Eng.*, Vol. 57-58, p. 327, 2001.
- [18] P. Laakkonen, J. Lautanen, M. Schirmer, and J. Turunen, "Multilevel diffractive elements in  $\text{SiO}_2$  by electron beam lithography and proportional etching with analogue negative resist", *J. Modern Opt.*, Vol. 46, No. 8, p. 1295, 1999.
- [19] P. Rai-Choudhury, "Handbook of microlithography, micromachining, and microfabrication", SPIE Optical Engineering Press, 1997.
- [20] S. Nonogaki, "Microlithography fundamentals in semiconductor devices and fabrication technology", Marcel Dekker Inc., 1998.
- [21] K. A. Valiev, "The physics of submicron litho-

- graphy”, Plenum press, 1992.
- [22] G. Messina, A. Paoletti, S. Santangelo, and A. Tucciarone, “Physical approximants to electron scattering”, *Microelectron. Eng.*, Vol. 34 p. 147, 1997.
  - [23] A. A Svintsov and S. I. Zaitsev, “Dose contribution of heating in electron-beam lithography”, *J. Vac. Sci. Technol. B*, Vol. 13, p. 2550, 1995.
  - [24] L. H. Veneklasen, “Optimizing electron beam lithography writing strategy subject to electron, optical, pattern, and resist constraints” , *J. Vac. Sci. Technol. B*, Vol. 9, p. 3063, 1991.
  - [25] M. Bai, R. F. W. Pease, C. Tanasa, M. A. McCord, D. S. Pickard, and D. Meisburger, “Charging and discharging of electron beam resist films”, *J. Vac. Sci. Technol. B*, Vol. 17, p. 2893, 1999.
  - [26] T. P. Pearsall, “Quantum semiconductor devices and technologies”, Kluwer Academic Publishers, 2000.
  - [27] M. Köhler, “Etching in microsystem technology”, Wiley-VCH, p. 144, 1999.
  - [28] S. Winkelmeier, M. Sarstedt, M. Ereken, M. Goethals, and K. Ronse, “Metrology method for the correlation of line edge roughness for different resists before and after etch”, *Microelectron. Eng.*, Vol. 57, p. 665, 2001.
  - [29] H. Ohki, T. Asari, H. Takemura, M. Isobe, and K. Moriya, “Fabrication of grating patterns by e-beam lithography”, *Microelectron. Eng.*, Vol. 9 p. 235, 1989.
  - [30] U. Klein and F. Götz, “Definition of geometries with complicated, curved boundaries for electron beam pattern generation”, *Microelectron. Eng.*, Vol. 9, p. 495, 1997.
  - [31] D. C. Lee and J. K. Park, “A study on the e-beam resist characteristics of plasma polymerized styrene”, *J. of KIEEME(in Korean)*, Vol. 7, No. 5, p. 425, 1994.
  - [32] S. G. Park, “Electric and electrochemical characteristic of PMMA-PEO gel electrolyte for rechargeable Lithium battery”, *J. of KIEEME(in Korean)*, Vol. 11, No. 10, p. 768, 1998.
  - [33] K. Shin and J. W. Kim, “The optical properties of amorphous germanium transmission grating”, *EID '99 digest paper*, p. 117, 1999.